Video Article

Multimodal Quantitative Phase Imaging with Digital Holographic Microscopy Accurately Assesses Intestinal Inflammation and Epithelial Wound Healing

Philipp Lenz[1,2], Markus Brückner[1], Steffi Ketelhut[3], Jan Heidemann[4], Björn Kemper*[3], Dominik Bettenworth*[1]

[1]Department of Medicine B, University Hospital Münster

[2]Institute of Palliative Care, University Hospital Münster

[3]Biomedical Technology Center, University of Münster

[4]Department of Gastroenterology, Klinikum Bielefeld

*These authors contributed equally

Correspondence to: Björn Kemper at bkemper@uni-muenster.de

URL: http://www.jove.com/video/54460
DOI: doi:10.3791/54460

Keywords: Medicine, Issue 115, Gastroenterology, digital holographic microscopy, quantitative phase imaging, label-free, stain-free, inflammation, wound healing, quantitative microscopy

Date Published: 9/13/2016

Citation: Lenz, P., Brückner, M., Ketelhut, S., Heidemann, J., Kemper, B., Bettenworth, D. Multimodal Quantitative Phase Imaging with Digital Holographic Microscopy Accurately Assesses Intestinal Inflammation and Epithelial Wound Healing. *J. Vis. Exp.* (115), e54460, doi:10.3791/54460 (2016).

Abstract

The incidence of inflammatory bowel disease, *i.e.,* Crohn's disease and Ulcerative colitis, has significantly increased over the last decade. The etiology of IBD remains unknown and current therapeutic strategies are based on the unspecific suppression of the immune system. The development of treatments that specifically target intestinal inflammation and epithelial wound healing could significantly improve management of IBD, however this requires accurate detection of inflammatory changes. Currently, potential drug candidates are usually evaluated using animal models *in vivo* or with cell culture based techniques *in vitro*. Histological examination usually requires the cells or tissues of interest to be stained, which may alter the sample characteristics and furthermore, the interpretation of findings can vary by investigator expertise. Digital holographic microscopy (DHM), based on the detection of optical path length delay, allows stain-free quantitative phase contrast imaging. This allows the results to be directly correlated with absolute biophysical parameters. We demonstrate how measurement of changes in tissue density with DHM, based on refractive index measurement, can quantify inflammatory alterations, without staining, in different layers of colonic tissue specimens from mice and humans with colitis. Additionally, we demonstrate continuous multimodal label-free monitoring of epithelial wound healing *in vitro*, possible using DHM through the simple automated determination of the wounded area and simultaneous determination of morphological parameters such as dry mass and layer thickness of migrating cells. In conclusion, DHM represents a valuable, novel and quantitative tool for the assessment of intestinal inflammation with absolute values for parameters possible, simplified quantification of epithelial wound healing *in vitro* and therefore has high potential for translational diagnostic use.

Video Link

The video component of this article can be found at http://www.jove.com/video/54460/

Introduction

Inflammatory bowel disease (IBD), *i.e.,* Ulcerative Colitis (UC) and Crohn's disease (CD) are idiopathic inflammatory disorders of the gastrointestinal tract[1]. Research into the underlying pathophysiology of IBD and the evaluation of potential new drugs or novel diagnostic approaches is particularly of importance. In both basic research and the clinical management of IBD patients, the intestinal mucosa has become a focus of attention[2,3]. The mucosa represents an anatomical boundary, at which the interaction between commensal bacteria, epithelial cells and various cellular components of the intestinal immune system orchestrate gut homeostasis[4,5]. However, in IBD patients, uncontrolled and persistent intestinal inflammation leads to mucosal damage, detectable as ulcerations or stenosis, which can finally culminate in breakdown of epithelial barrier function, which itself aggravates local inflammation[6].

Epithelial wound healing is therefore crucial for epithelial regeneration following inflammation but is also a core requirement for the healing of gastrointestinal ulcers or anastomotic leakage after gastrointestinal surgery[7]. Epithelial wound healing can be simulated in *in vitro* wound healing assays and in murine models of intestinal inflammation[8,9]. Both *in vitro* and *in vivo* approaches have drawbacks, which limit the accuracy of experimental assessment. *In vitro* assays, like classical scratch assays, require protracted staining procedures or transfection with fluorescent chromophores. They are often limited by their discontinuous monitoring of cell proliferation and migration that cannot be automated[10]. *In vivo* models, such as dextran sodium sulphate (DSS)-induced colitis, frequently lack robust read-outs, in part due to the significant variation seen in laboratory markers, making such markers inappropriate to evaluate colitis severity[11,12]. Histological analysis of the inflamed mucosa is currently still the most valid approach to determine colitis severity but this, like *in vitro* epithelial wound healing assays, requires staining and is dependent on investigator's expertise[13].

Recently digital holographic microscopy (DHM), a variant of quantitative phase microscopy[14], was identified as useful tool for the evaluation of epithelial wound healing *in vitro* and *in vivo*[15]. DHM allows assessment of tissue density by measuring optical path length delay (OPD), which prospects novel cancer diagnosis[16-18] and quantification of inflammation related tissue alterations[19]. Additionally, DHM allows monitoring of cell morphology dynamics by determining cell thickness, cell covered surface area and intracellular (protein) content quantity[15,20]. In *in vitro* assays, DHM also enables the analysis of physiological processes, *e.g.,* cellular water permeability by evaluating changes in cell volume and thickness[21,22]. Moreover, DHM measurements can be automated which prevents investigator-associated sample bias.

Here, we demonstrate the use of DHM in a murine model of intestinal inflammation, and also apply DHM to analysis of human tissues samples for quantitative monitoring of wound healing as a label-free *in vitro* assay. First, we evaluate inflammatory alterations of different colonic wall-layers in colitic mice and tissue sections from humans with IBD. After describing the DHM quantitative phase imaging procedure, we provide detailed instructions for using the microscope components, the preparation of tissue sections and also describe the evaluation of the acquired quantitative phase images.

Next, we show that DHM can be utilized for continuous multimodal monitoring of epithelial wound healing *in vitro*, and describe the analysis of cellular characteristics like cell layer thickness, dry mass and cellular volume give insight into drug induced and physiologic cell alterations.

Protocol

All animal experiments were approved by the regional ethics committee (the Landesamt für Natur, Umwelt und Verbraucherschutz, LANUV, Germany) according to German Animal Protection Law. The local ethics committee of the University of Münster approved the use of human tissues for histological and microscope analysis.

1. Animals and Materials

1. Use female or male mice of the required DSS-susceptible strain that weigh 20 to 25 g, and house according to local animal care legislation. Provide special chow for rodents and autoclaved drinking water *ad libitum*.
2. Induce *acute* DSS colitis by administering 3% w/v dextran sulfate sodium (DSS, molecular weight: 36,000-50,000 Da) in autoclaved tap water for 5 days.
   NOTE: The potency of DSS is highly variable depending on manufacturer and batch. Test your supplier-provided DSS first for induction of disease activity, for which daily body weight is a reliable and objective indicator.
3. For histological evaluation of colonic tissue samples, euthanize mice by CO_2 insufflation (or as specified by national and institutional guidelines) at the end of the experiment.

2. Experimental Setup for DSS-colitis and *In-vitro* Wound Healing Assays

1. Cell culture and establishment of wound healing assay.
   1. Grow Caco-2 cells in a 95% humidity and 5% CO_2 environment at 37 °C. Use RPMI medium with 10% fetal bovine serum (FBS) and 1% penicillin/streptomycin.
   2. Seed Caco-2 cells at a density of 4 x 10^5 cells/cm^2 on 35 mm Petri dishes with high culture-insert (see **Figure 4A**).
      NOTE: The insert generates two cell covered areas that are separated with a defined cell free space representing the wounded area to be analyzed.
   3. Change medium two days after seeding. Perform by first aspirating residual medium with cell debris by using an automatic pipette, rinse with 100 µl of phosphate buffered saline (PBS) and add fresh RPMI medium or serum-deprived medium.
   4. Culture cells for 24 hr in serum-deprived medium (0.1% FBS) supplemented with 20 ng EGF/ml serum or 2 µg mitomycin c/ml serum to detect alterations in wound healing behavior. Add normal RPMI medium to control cells for 24 hr.
   5. After 24 hr of culture, remove and discard culture inserts as described in step 3.4 and perform DHM.

2. Induction of acute DSS colitis
   1. Dissolve 3 g of DSS in 100 ml autoclaved water to get a 3% (w/v) DSS solution. Provide this solution in place of drinking water to mice *ad libitum* for 7 days. Calculate 5 ml of DSS-solution per mouse/day. Provide autoclaved water without DSS for control mice *ad libitum*.

3. Preparation of cryostatic sections of murine and human colon
   1. Euthanize mice by CO_2 insufflation at the end of the experiment.
   2. Dissect the animals' abdomen by laparotomy[23]. Remove the whole colon carefully using tweezers and cut the ileal and rectal end using surgical scissors. Cut the colon with a scissors longitudinally from the cecal to the rectal end and open the colon. Remove all feces from the specimen using tweezers followed by washing with PBS[24].
   3. Prepare Swiss rolls by rolling up the whole colon with a cotton bud longitudinally from the cecal to the rectal end with the mucosa curved inwards. Embed colonic samples in optimal cutting temperature (OCT) compound and keep frozen at -80 °C until further use.
   4. Embed human colonic tissue from surgical specimen in optimal cutting temperature OCT compound and keep frozen at -80 °C until further use.
   5. Cut sections of 7 µm thickness of the OCT-compound-embedded specimens with the help of a cryotome just prior to examination.
      NOTE: The optimum sample thickness depends on the persistence and the scattering properties of the tissue type under investigation. For the described experiments using colon tissue, slice thickness > 10 µm cause significant increase in noise due to light scattering in quantitative DHM phase contrast images, while samples of thickness < 5 µm show a higher risk for damage induced artefacts from the cryo cutting process.
   6. Transfer sections on to a glass object carrier slide.

3. Technical Equipment, Software and Procedures for Acquisition and Evaluation of Digital Holograms

1. Digital holographic microscope for quantitative cell and tissue imaging
    1. Use an off-axis Mach-Zehnder digital holographic microscopy system for live cell imaging[25], as shown in **Figure 1**. Ensure that the microscope is equipped with a 10X microscope lens, a microscope stage with a holder for glass object carrier slides and Petri dishes with a diameter of 35 mm, a heating chamber to preserve physiological temperature at 37 °C and software for quantitative phase imaging[25].
    NOTE: For example, as described in Kemper *et al.*[26] and Langehanenberg *et al.*[27].
    NOTE: Alternatively, use a similar system that is capable of performing bright field microscopy and quantitative phase imaging of living cells and dissected tissue slides.
    2. Clean microscope lens and condenser with lens cleaning paper and a cleaning agent (*e.g.,* ethanol) as recommended by the manufacturer of the microscope to remove dust or other contaminations.
    3. Start the image acquisition software of the DHM microscope, select "bright field" imaging mode and switch "on" white light illumination. Ensure Köhler-illumination of the sample as recommended by the microscope manufacturer while observing the sample in the live imaging window of the image acquisition software (alternatively a standard image acquisition software can be used in this step).
    NOTE: The image intensity should be distributed homogeneously in the field of view and the sample position should not move during optical refocusing with the focus drive of the microscope.
    4. Select "DHM" imaging mode, turn "off" white light illumination and switch "on" the laser light. Check that the illumination with laser light is homogeneous (*i.e.*, that light intensity is homogeneously distributed in the live imaging window of the imaging acquisition software of the DHM microscope) and observe that the off-axis carrier interference fringe pattern appears with adequate contrast in the captured images (digital holograms).

2. Preparation of cryostat sections for imaging with DHM
    1. Take the sample (cryostat section on a glass object carrier, thickness: 7 µm, as described in 2.3) out of the freezer. Defrost the sample for about 5 min at RT and normal atmosphere.
    2. Add 50 - 100 µl phosphate buffered saline (PBS) as embedding medium onto the tissue section using a pipette until it is completely covered with buffer. Cover the sample with a clean glass cover slip (glass thickness 170 µm).
    NOTE: Over-drying can induce significant changes of the refractive index and scattering properties of the sample.
    3. Ensure that the bottom of the glass carrier and the cover slip are cleaned from dust and other contamination that may induce light scattering. The sample is ready for investigation with bright field microscopy and DHM.

3. Quantitative phase imaging of tissue sections with DHM
    1. Switch on the digital holographic microscope, choose the 10X microscope lens for imaging. Start the image acquisition software of the DHM microscope and select bright file imaging mode.
    2. Place the tissue slide as described in 2) in the microscope slide holder, with the cover slip facing the microscope objective.
    3. Switch "on" the bright field illumination of the DHM microscope. Position the sample with the microscope stage and ensure that the tissue area of interest is visible in the live monitoring window. Improve the sharpness of the image using the microscope's focus drive.
    NOTE: As well as the area of interest, an area of slide without tissue should also be present in the field of view.
    4. Capture a bright field image of the sharply focused sample using the image acquisition software.
    5. Select "DHM" imaging mode, turn "off" the white light illumination and turn "on" the laser light illumination. Select the "exposure time" for hologram recording below 3 msec, observe that holographic off-axis interference fringes appear with adequate contrast in the live imaging window of the imaging acquisition software and capture a digital hologram.
    6. Repeat steps 3.3.3 - 3.3.5 until a sufficient number of bright field images and digital holograms of different sample areas have been recorded. Hologram acquisition is now complete.

4. Preparation of wound healing assays for DHM imaging
    1. Switch on the Petri dish heating chamber of the DHM microscope about 1 - 3 hr prior to the start of the experiment to ensure stable temperature conditions during the DHM measurements.
    2. Prepare workbench with the required equipment (Petri dish for wound healing assay is described in 2.3): pipettes, tweezers, glass lid for Petri dish, 4-(2-hydroxyethyl)-1-piperazineethanesulfonic acid (HEPES) buffered cell culture medium with physiological temperature (37 °C) for sample preparation in sterile environment.
    NOTE: Dulbecco's Modified Eagle Medium (DMEM) is composed of 10 % fetal calve serum (FCS), 20 mM HEPES (4-(2-hydroxyethyl)-1-piperazineethanesulfonic acid), and 850 mg/L $NaHCO_3$.
    3. Remove the plastic lid from the Petri dish and remove the cell culture medium with a pipette. Remove the insert from the Petri dish bottom using tweezers.
    4. Wash the sample 1 - 2 times with 1 ml HEPES buffered cell culture medium in order to remove dead cells and remaining cellular components (*e.g.*, serum) in the wound area. Add 2 ml HEPES buffered cell culture medium and cap the Petri dish with the glass lid.
    5. Ensure that the glass lid and the Petri dish bottom have been cleaned from dust and other contamination. Sample is ready for time lapse observation with DHM.

5. Continuous multimodal monitoring of wound healing *in vitro* with DHM
    1. Switch on the Petri dish heating chamber of the DHM microscope about 1 - 3 hr prior to the start of the experiment to ensure stable temperature conditions during the DHM measurements.
    2. Switch "on" the digital holographic microscope, select the 10X microscope lens for imaging. Start the image acquisition software of the DHM microscope and select "bright field" imaging mode. Ensure that the heating chamber for the Petri dish is operating a physiological temperature (37 °C).
    3. Place the Petri dish with the wound healing assay, prepared as described in 4), in the heating chamber of the DHM microscope.

4. Select bright field imaging mode and position the sample with the microscope stage while observing it in the live monitoring window of the image acquisition software of the DHM microscope. Observe that the desired area of the sample appears sharply focused under white light illumination.
5. Capture bright field images of different areas of the sample (wound area and surrounding areas with confluent cells) under white light illumination with the image acquisition software and document appearance, cell density and homogeneity.
6. Select "bright field" imaging mode of the DHM microscope. Choose a suitable wound area under white light illumination in the live monitoring window with the image acquisition software of the DHM microscope. Ensure the wound area is free from dead cells and no serum remains, and ensure that both sides include a single homogeneous cell layer, preferably with straight borders.
7. Capture a white light image of the initial wound area in bright field imaging mode with the image acquisition software of the DHM microscope.
8. Turn "off" white light illumination, select "DHM" mode and switch "on" laser illumination. Select an exposure time of below 3 msec for hologram recording (observe that holographic off-axis interference fringes appear with adequate contrast in the live imaging window of the image acquisition software of the DHM microscope) and capture a digital hologram.
9. Capture a sample hologram in DHM mode with the image acquisition software and reconstruct a quantitative phase image with the reconstruction software of the DHM microscope in order to check the image quality.
10. Select a suitable time delay (*e.g.*, 3 - 5 min) for time-lapse hologram acquisition with the image acquisition software of the DHM microscope.
11. Select the time-lapse acquisition mode of the image acquisition software in which the sample is only illuminated with laser light during hologram acquisition.
12. Start the time-lapse DHM observation of the wound healing assay.
13. Stop the time-lapse acquisition after the intended time, select bright field imaging mode and document the final appearance of the sample under white light imaging.

6. Reconstruct digital holograms of dissected tissues and determine the average refractive index as a parameter to quantify tissue density
   1. Reconstruct quantitative phase images from the digital holograms of dissected tissues with the software of the DHM microscope, *e.g.*, as described in Kemper *et al.*[26] and Langehanenberg *et al.*[27].
   2. Determine the average phase contrast Δφ in different tissue layers (epithelium, submucosa, stroma) in appropriately chosen regions of interests (ROIs)[19].
   3. Determine the refractive index of the embedding medium by using a refractometer or alternatively by using an appropriate value from the literature. (refractive index values for typical embedding media: n_{water} = 1.334 [28], $n_{Phosphate\ buffered\ saline\ (PBS)}$ = 1.337 [29], $n_{cell\ culture\ medium}$ = 1.337-1.339 [29,30]).
   4. Calculate the refractive indices of different tissue layers from the average phase contrast values[19]

$$n_s = \left(\frac{\Delta\varphi_s}{d} \frac{\lambda}{2\pi} \right) + n_{medium} \quad (1)$$

NOTE: In Eq. 1 λ is the wavelength of the laser light (here: λ = 532 nm), *d* the thickness of the dissected tissues (here: 7 µm) and n_{medium} is the refractive index of the embedding medium (here: $n_{medium} = n_{PBS}$ = 1.337, determined by an Abbe-Refractometer).

7. Reconstruct and evaluate digital holograms from the time-lapse wound healing series observation
   1. Reconstruct quantitative phase images from the time lapse hologram series obtained during wound healing observation with the DHM microscope software[26,27].
   2. Normalize each series of quantitative phase images to the image with maximum phase contrast.
   3. Determine the area S_c that is covered by the cells in the quantitative DHM phase images by image segmentation, which can be performed using the free software cell profiler (www.cellprofiler.org[31]).
   4. Calculate the average phase contrast of the cells $\Delta\varphi_{cell}$ in the area S_c.
   5. Retrieve the cellular dry mass DM from the average phase contrast $\Delta\varphi_{cell}$ in the area S_c[15]

$$DM = \frac{10\lambda}{2\pi\alpha} \Delta\varphi_{cell} S_c \quad (2)$$

NOTE: In Equation 2 DM denotes the cellular dry mass, S_c presents the area that is occupied by the cells and α = 0.002 m^2/kg.
   6. Determine the integral cellular refractive index n_{cell} and the refractive index of the cell culture medium n_{medium}. Determine n_{cell} separately experimentally from suspended cells as described in [30] and measure n_{medium} with a refractometer. Alternatively use literature values for n_{cell} [30] and n_{medium} [29,30].
   7. Calculate the average cell thickness d_{cell} from λ, $\Delta\varphi_{cell}$, n_{cell} and n_{medium} [26,32]

$$d_{cell} = \frac{\lambda}{2\pi(n_{cell} - n_{medium})} \Delta\varphi_{cell} \quad (3)$$

NOTE: In Eq. 3 the parameter d_{cell} is the average cell thickness, λ denotes the light wavelength of the laser light, $\Delta\varphi_{cell}$ denotes the average phase contrast, and n_{cell} and n_{medium} are the integral cellular refractive index and the refractive index of the surrounding medium.

Representative Results

Typical Setup for DHM Imaging for Digital Holographic Microscopy (DHM)

To perform bright field imaging and quantitative DHM phase contrast imaging, we applied an inverted microscope as depicted in **Figure 1B**. The system was modified by attaching a DHM module, as described earlier[25]. Digital holograms were generated by illumination the sample with the light of a frequency-doubled Nd:YAG laser λ = 532 nm) in Mach-Zehnder configuration (**Figure 1A**). Dissected tissues were analyzed *ex vivo* on glass carrier slides. Living cell cultures were observed in special Petri dishes for observing wound healing as shown in **Fig. 1C**. The samples were imaged in transmission illumination via a 10X microscope lens (NA = 0.3) and a tube lens. A charge-coupled device camera was used to record the interference patterns (digital off-axis holograms) generated by superimposing the sample image (object wave) with the slightly tilted reference wave. The digitally captured holograms were reconstructed by spatial phase shifting reconstruction in combination with optional holographic autofocusing[26,33].

Assessment of Murine DSS-induced Colitis by DHM

Acute colitis was induced in mice by administration of 3% w/v dextran sulfate sodium (DSS) in drinking water for 5 days. The manifestation and course of colitis was followed by monitoring for progressive weight loss in the DSS-treated group compared to the control group. (**Figure 2A** adapted from [19]). Endoscopically, moderate to severe colitis was observed as reflected by thickening of the colonic wall, alterations of the vascular pattern (*e.g.,* spontaneous bleeding, *red arrow*), fibrin exudations (*white arrow*) and granularity of the mucosal surface (**Figure 2B**). Conventional histological evaluation of hematoxylin and eosin (HE) stained colonic sections revealed marked edema in the colonic wall of DSS-treated verses control animals, predominantly located in the submucosa (**Figure 2C** *gray arrow*). Corresponding quantitative DHM phase contrast images and related refractive index maps retrieved by Equation 1, also depicted the above-mentioned tissue alterations. Additionally, the refractive index, coded to 256 gray levels, indicated differences in density in tissue layers including the epithelium (*white arrow*) and stroma (*black arrow*) in native, unstained tissue samples (**Figure 2C**). The refractive index was significantly reduced in the epithelium, as well as in the submucosa and stroma of the colitic mice compared to the healthy controls (**Figure 2E**). Additionally, a significant correlation between the clinical parameter (relative loss of body weight) and the absolute physical parameter (refractive index) could be observed (R^2 linear = 0.64; **Figure 2D,** adapted from [19]).

Assessment of Crohn's Disease in Humans by DHM

Crohn's disease is often identified by remarkable inflammatory alterations of the intestinal wall, detected by gastrointestinal endoscopy. Characteristic macroscopic features comprise of granularity of the mucosal surface, longitudinal ulcers with fibrin exudations (also referred to as "snail trails") and spontaneous bleeding (**Figure 3A**). Histological evaluation by HE staining of tissue samples from patients with active CD often reveal colonic wall as well as submucosal edema. Corresponding quantitative DHM phase contrast images and related refractive index maps retrieved by Equation 1 also detected inflammatory-mediated enhancement/swelling of the colonic wall, here seen in the epithelium (**Figure 3B**). Furthermore, the refractive index as an absolute parameter, was also significantly reduced in all wall layers (epithelium, submucosa and stroma) in colonic tissue samples from patients with active CD verses those in remission (**Figure 3C**).

Multimodal Monitoring of Wound Healing *In-vitro*

Caco-2 cell wound healing assays were performed using a special Petri dish to provide standardized conditions. The dish is equipped with a culture insert forming two different chambers, which are separated by a gap of 500 µm (**Figure 4A**). To simulate different physiological environments, cells were examined either without treatment, stimulated by epidermal growth factor (EGF) or inhibited with Mitomycin c. The DHM setup allows continuous monitoring of the wound healing process over time, depicted here by representative quantitative DHM phase contrast images (coded to 256 gray levels) after 0, 22.5 and 45 hr after the start of the experiment (**Figure 4B**). Corresponding false color-coded pseudo 3D plots **in Figure 5** illustrate the spatial development of the cell layer thickness in three dimensions. Based on the optical path length delay, the cellular refractive index and equations 2 and 3, DHM allows simultaneous dynamic assessment of migration, proliferation and morphology by temporal monitoring of cellular characteristics such as cell covered surface area, average cell thickness and cellular dry mass (**Figure 4C**). In summary, the data in **Figure 4** illustrate that EGF simulation results in a faster migration of cells into the wound area, in an increased average cell thickness and in a higher dry mass in the field of view compared to control cells. In contrast, Mitomycin c inhibited cells cover a slightly decreased surface area than control cells during the course of the experiment and show also a slightly lower dry mass increase. However, the average cell thickness appears clearly decreased compared to both, stimulated and control cells.

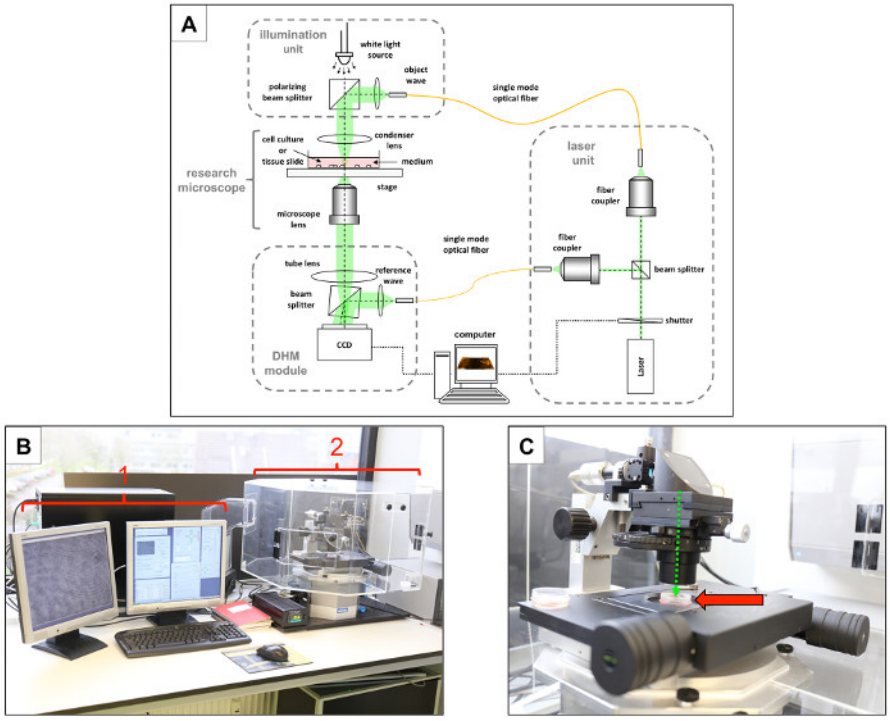

Figure 1. Utilized Off-axis Setup for Digital Holographic Microscopy (DHM). Schematic setup of the DHM workstation **(A)**. Corresponding photograph depicting the microscope setup (monitor, live image and control software (1), off-axis setup digital microscope (2), **(B),** the optical path of the microscope (*green dotted line*) and a sample (indicated by *red arrow*; **(C)**). Please click here to view a larger version of this figure.

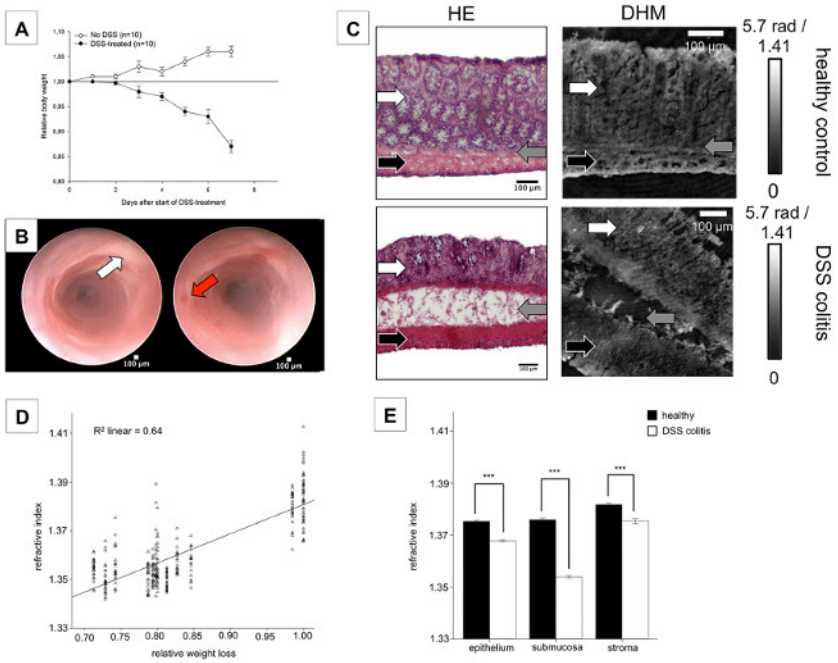

Figure 2. Assessment of Murine DSS-induced Colitis by DHM. The course of colitis was followed by daily measurement of relative body weight and repeated endoscopic follow-up examination. A massive loss of relative body weight from day 4 after start of DSS administration (adapted from[19]) (**A**) was accompanied by endoscopic signs of established colitis including focal ulcerations and mucosal vulnerability (**B**). Analysis of conventional HE-stained cryostatic sections revealed submucosal edema, thickening of the muscularis and a pronounced mucosal inflammatory infiltrate in the mucosa. Corresponding quantitative DHM phase contrast images and related refractive index maps retrieved by Equation 1 (coded to 256 gray levels) confirmed the edematous changes of the submucosa during the inflammatory process (white arrow indicates epithelium, grey submucosa and black stroma) (**C**). The relative loss of body weight (a clinical parameter) significantly correlated with the refractive index (an absolute physical parameter, R^2 linear = 0.64; (**D**), adapted from[19]), which was significantly reduced in the epithelium as well as in the submucosa and stroma of the colitic mice compared to the healthy controls (mean ± SEM, *** P < 0.001; **E**). Please click here to view a larger version of this figure.

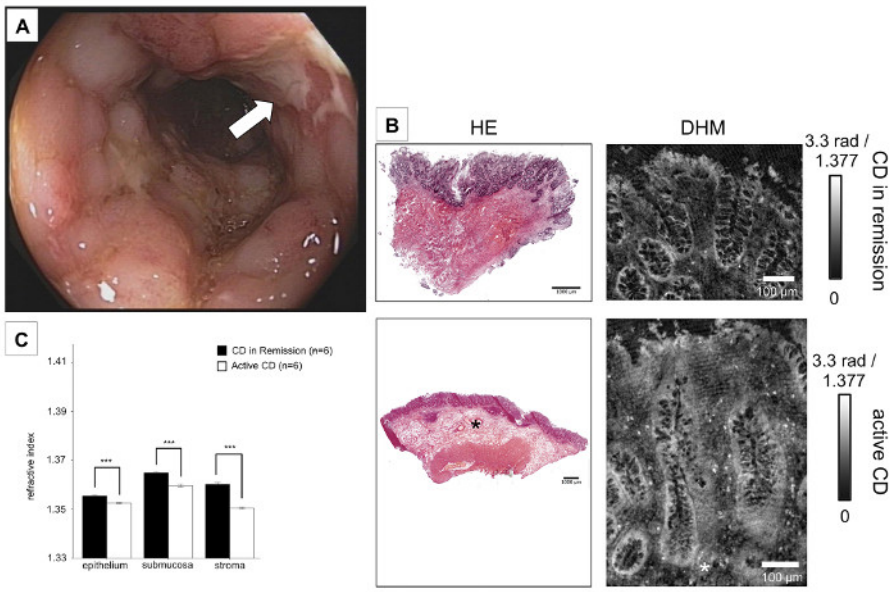

Figure 3. Assessment of Crohn's Disease in Humans by DHM. Colonic tissue samples from patients with endoscopically and histologically confirmed Crohn's disease were examined (**A**). HE-staining displayed lengthening of mucosal crypts and a marked infiltrate of inflammatory cells. Furthermore, submucosal edema and enlargement of the muscularis propria was detected. Analysis of corresponding quantitative DHM phase contrast images and related refractive index maps retrieved by Equation (1) (coded to 256 gray levels) also revealed edematous changes (here indicated by a *white and black star*) in the epithelium (**B**). Significant differences in average refractive index were detected in samples from CD patients with active flare (*clear bars*) or remission(*black bars*). These differences are seen in each tissue type (mean ± SEM, ***P < 0.001; **C**). Please click here to view a larger version of this figure.

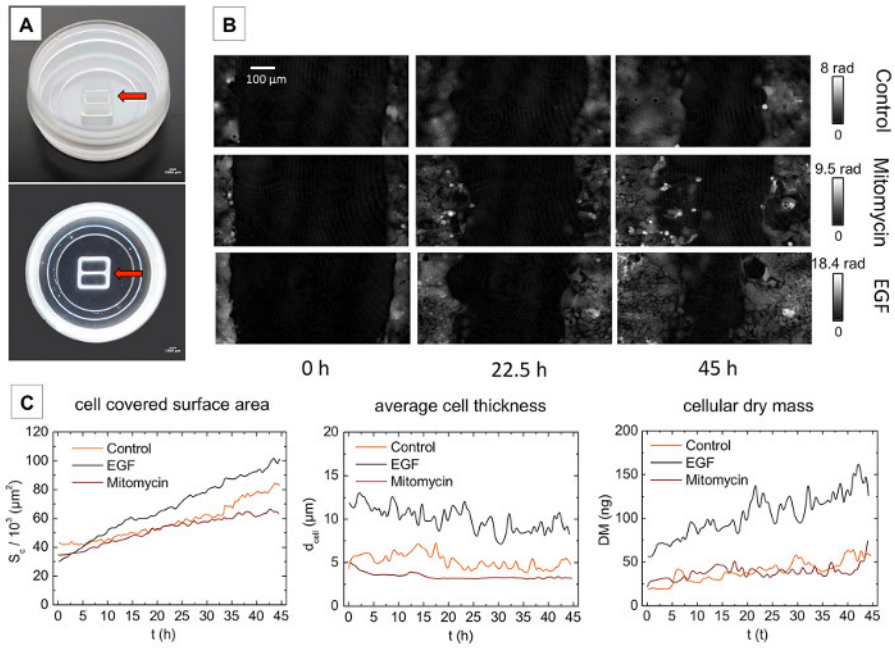

Figure 4. Monitoring of Epithelial Wound Healing by White Light Microscopy and DHM. Cultured cells were transferred into Petri dishes with special inserts (*red arrow*). Before culture inserts were removed, cells were treated with either EGF or Mitomycin c for 24 hr, or treated with medium alone (unstimulated control) (**A**). After removal of culture inserts, wound healing was continuously monitored by phase contrast imaging by DHM over time. Cell outlines could be clearly recognized. Representative quantitative DHM phase contrast images are shown at the beginning of the experiment, after 22.5 hr and at the end of the measurement after 45 hr (**B**). Panel (**C**) shows the corresponding temporal changes in the cell-covered surface (S_c), the average cell thickness (d_{cell}) and the cellular dry mass (*DM*). Please click here to view a larger version of this figure.

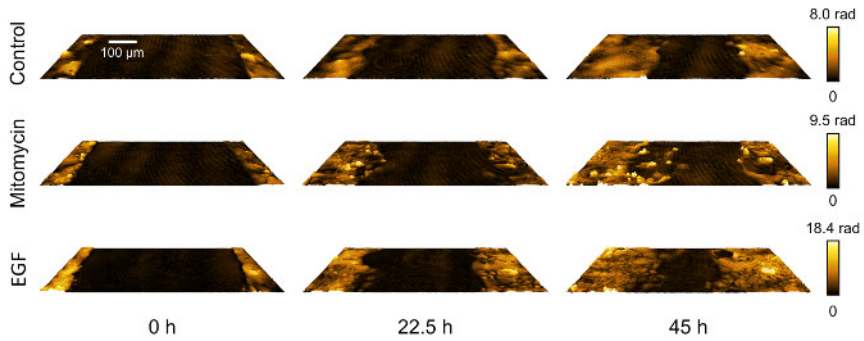

Figure 5. Illustration of Cell Layer Morphology Changes by False Color-coded Pseudo 3D Plots of the Quantitative DHM Phase Contrast Images. Representative false color-coded pseudo 3D plots of the quantitative DHM phase contrast images in **Figure 4B** at t = 0, after 22.5 hr and at the end of the measurement after 45 hr, illustrate spatial development of the thickness of cell layers for control-, Mitomycin c-inhibited and EGF-stimulated cells in 3D. Please click here to view a larger version of this figure.

Discussion

We demonstrate that DHM provides accurate assessment of histological damage in murine colitis models and human colonic tissue samples *ex vivo*. Furthermore, we shown DHM can continuously monitor epithelial wound healing whilst simultaneously providing multimodal information about cellular alterations. In DHM, the reconstruction of digitally captured holograms is performed numerically[32]. Therefore, in comparison to bright field microscopy, Zernike phase contrast and differential interference contrast microscopy, DHM provides quantitative phase contrast with optional subsequent numerical focus correction (multi-focus imaging)[27]. Quantitative phase imaging is based on the determination of optical path length changes and thus is highly independent of the measurement device utilized. This simplifies the comparison of measurement data that are acquired with different instruments. In addition, DHM requires only low light intensity for object illumination. This enables a minimally invasive analysis of unstained dissected tissues and minimizes the amount of sample interaction required during long-term time-lapse observations of living cells.

The therapeutic armamentarium for IBD has significantly broadened over the two last decades. Besides the introduction of anti TNF-α therapies, which are effective in both UC and CD and have acceptable side-effect profiles, novel and specific antibodies targeting integrins were recently introduced into clinical practice[34-37]. Several other promising agents are currently being evaluated for their therapeutic efficacy in IBD[38-40]. However, prior to the clinical use in humans, the efficacy and safety of these potential therapies has to be proven in animal studies. The DSS-induced colitis is one of the most frequently used murine colitis models, due to its high reproducibility and low costs[23]. Additionally, this model can also be applied to genetically altered mice strains[41]. While systemic markers, *e.g.,* CRP, are highly variable in animal models, histological assessment of the colon represents the most valid approach to assess disease severity[42,43]. Nevertheless, quantitative evaluation of histological inflammation according to scoring systems is highly dependent on investigator expertise and experience. Automated assessment and scoring by objective parameters as possible with DHM overcomes these limitations, and furthermore is also time-saving, avoiding the need for staining[19]. Furthermore, DHM may be used to examine surgical colonic specimens as well as mucosa samples obtained during endoscopy.

Epithelial regeneration and wound healing is a pivotal mechanism during several pathological process including gastrointestinal ulceration or anastomotic leakage. While there are promising approaches to assess epithelial wound healing *in vivo*[44], these techniques require sophisticated examination tools and are currently not widely available. Therefore, currently epithelial healing is commonly investigated by scratch assays *in vitro*[9]. These assays allow valid examination of wound closure but usually first require the cell staining, which then prevents repeated evaluation[10,45]. In addition, no cellular alteration data can be acquired in parallel with this experimental setup. However, this information may be of significant importance since it can be used to differentiate between apoptosis and necrosis[46] and to assess cell proliferation and migration[46]. Therefore, the possibility to determine cell thickness, dry mass or tissue density simultaneously to the monitoring of wound closure by DHM examination is of high value in mucosal research.

Treatment goals for human IBD patients have been constantly changing over the last decades[47]. While initially the control of inflammation was regarded to be of primary importance, later steroid-free remission and now mucosal healing are primary goals of treatment[48]. Recently, it was hypothesized that histological remission may even be superior to mucosal healing alone[49]. However, whilst there are a few histological scoring systems available for human IBD, the inter-observer variability remains high[50]. Therefore, there is a need for a standardized approach for the evaluation of histological colonic samples. DHM may contribute to this goal and should be further evaluated in a prospective clinical trial with human IBD patients.

In the experimental procedure presented, the samples are illuminated and imaged using highly coherent laser light. Therefore, the resolution in DHM is mainly limited by light scattering and diffraction effects caused by misalignment of the sample illumination, thick samples, dust or other impurities such as condensed water in the optical path. In order to achieve highly precise measurement data from quantitative DHM phase contrast images, careful preparation and alignment of the DHM setup and the sample are the most important steps in the protocol. Thoroughly cleaned optical imaging elements, in particular the microscope condenser and microscope objective, are required to minimize noise. Also sample carrier slides, Petri dish lid and bottom, as well as the utilized cell culture medium should be free from particulate impurities. This is achieved by carefully cleaning all components and adequate filtering of the applied liquids.

More detailed trouble shooting tips are as follows: if the digital hologram and/or the quantitative DHM phase images of dissected tissues are noisy, the glass carrier and cover slip may be contaminated with dust. If so, clean the glass carrier and cover slip with alcohol (*e.g.,* pure ethanol). If the thickness of dissected tissue is too large (> 10 µm) and thus results in light scattering, try using thinner tissue sections. In the

event that the illumination with laser light is not homogeneously distributed, align the object illumination via the microscopes condenser. If condensed water on the bottom of the glass lid induces scattering effects, check the temperature of the heating chamber and room humidity. In case the cell density is too high or cell growth in more than one layer, reduce the cell density during preparation of wound healing assays. Finally, as DHM is based on the principle of interferometry, the method is sensitive to vibrations or other mechanical disturbances, which vary according to the individual laboratory environment. However, such influences usually can be minimized by adequately chosen exposure times (typically in millisecond range or below) for holography recording during the preparation of the experimental setup.

In summary, our results demonstrate that DHM holds major advantages over bright field and existing phase contrast imaging microscopy techniques such as Zernike phase contrast and DIC due to its ability to quantitatively assess histological inflammation *ex vivo* in an almost automated fashion. Furthermore DHM allows label-free continuous multimodal evaluation of epithelial wound healing *in vitro* with minimized interaction with the samples. This paves the way to automated histological examination in terms of "digital pathology" and further extended studies to explore the translational potential of DHM on patients with IBD. In addition, DHM offers novel *in-vitro* opportunities to quantitatively study cell migration, morphology and proliferation.

The translation of DHM into clinical practice has the potential to improve IBD diagnostics. As DHM allows the quantification of different degrees of intestinal inflammation *via* physical parameters like density changes, an objective and more precise assessment of the disease in the sense of a "digital pathology" seems possible. The objective assessment can have an important impact on the clinical management of IBD patients.

Disclosures

The authors have nothing to disclose.

Acknowledgements

We thank Faekah Gohar for proofreading the manuscript. We thank Sonja Dufentester and Elke Weber for expert technical assistance.

References

1. Baumgart, D. C., & Sandborn, W. J. Inflammatory bowel disease: clinical aspects and established and evolving therapies. *Lancet.* **369**(9573), 1641-1657 (2007).
2. Dieleman, L. A. *et al.* Chronic experimental colitis induced by dextran sulphate sodium (DSS) is characterized by Th1 and Th2 cytokines. *Clin Exp Immunol.* **114**(3), 385-391 (1998).
3. Florholmen, J. Mucosal healing in the era of biologic agents in treatment of inflammatory bowel disease. *Scand J Gastroenterol.* **50**(1), 43-52 (2015).
4. Merga, Y., Campbell, B. J., & Rhodes, J. M. Mucosal barrier, bacteria and inflammatory bowel disease: possibilities for therapy. *Dig Dis.* **32**(4), 475-483 (2014).
5. Young, V. B., Kahn, S. A., Schmidt, T. M., & Chang, E. B. Studying the Enteric Microbiome in Inflammatory Bowel Diseases: Getting through the Growing Pains and Moving Forward. *Front Microbiol.* **2** 144 (2011).
6. Atreya, R., & Neurath, M. F. IBD pathogenesis in 2014: Molecular pathways controlling barrier function in IBD. *Nat Rev Gastroenterol Hepatol.* **12**(2), 67-68 (2015).
7. Jones, M. K., Tomikawa, M., Mohajer, B., & Tarnawski, A. S. Gastrointestinal mucosal regeneration: role of growth factors. *Front Biosci.* **4**D303-309 (1999).
8. Burk, R. R. A factor from a transformed cell line that affects cell migration. *Proc Natl Acad Sci U S A.* **70**(2), 369-372 (1973).
9. Singh, A., Nascimento, J. M., Kowar, S., Busch, H., & Boerries, M. Boolean approach to signalling pathway modelling in HGF-induced keratinocyte migration. *Bioinformatics.* **28**(18), i495-i501 (2012).
10. Sakalar, C. *et al.* Pronounced transcriptional regulation of apoptotic and TNF-NF-kappa-B signaling genes during the course of thymoquinone mediated apoptosis in HeLa cells. *Mol Cell Biochem.* **383**(1-2), 243-251 (2013).
11. Serada, S. *et al.* Serum leucine-rich alpha-2 glycoprotein is a disease activity biomarker in ulcerative colitis. *Inflamm Bowel Dis.* **18**(11), 2169-2179 (2012).
12. Turovskaya, O. *et al.* RAGE, carboxylated glycans and S100A8/A9 play essential roles in colitis-associated carcinogenesis. *Carcinogenesis.* **29**(10), 2035-2043 (2008).
13. Perse, M., & Cerar, A. Dextran sodium sulphate colitis mouse model: traps and tricks. *J Biomed Biotechnol.* **2012** 718617 (2012).
14. Lee, K. *et al.* Quantitative phase imaging techniques for the study of cell pathophysiology: from principles to applications. *Sensors (Basel).* **13**(4), 4170-4191 (2013).
15. Bettenworth, D. *et al.* Quantitative stain-free and continuous multimodal monitoring of wound healing in vitro with digital holographic microscopy. *PLoS One.* **9**(9), e107317 (2014).
16. Sridharan, S., Macias, V., Tangella, K., Kajdacsy-Balla, A., & Popescu, G. Prediction of prostate cancer recurrence using quantitative phase imaging. *Sci Rep.* **5** 9976 (2015).
17. Wang, Z., Tangella, K., Balla, A., & Popescu, G. Tissue refractive index as marker of disease. *J Biomed Opt.* **16**(11), 116017 (2011).
18. Majeed, H. *et al.* Breast cancer diagnosis using spatial light interference microscopy. *J Biomed Opt.* **20**(11), 111210 (2015).
19. Lenz, P. *et al.* Digital holographic microscopy quantifies the degree of inflammation in experimental colitis. *Integr Biol (Camb).* **5**(3), 624-630 (2013).
20. Popescu, G. *et al.* Optical imaging of cell mass and growth dynamics. *Am J Physiol Cell Physiol.* **295**(2), C538-544 (2008).
21. Klokkers, J. *et al.* Atrial natriuretic peptide and nitric oxide signaling antagonizes vasopressin-mediated water permeability in inner medullary collecting duct cells. *Am J Physiol Renal Physiol.* **297**(3), F693-703 (2009).
22. Jourdain, P. *et al.* Determination of transmembrane water fluxes in neurons elicited by glutamate ionotropic receptors and by the cotransporters KCC2 and NKCC1: a digital holographic microscopy study. *J Neurosci.* **31**(33), 11846-11854 (2011).

23. Wirtz, S., Neufert, C., Weigmann, B., & Neurath, M. F. Chemically induced mouse models of intestinal inflammation. *Nat Protoc.* **2**(3), 541-546 (2007).
24. Bettenworth, D. *et al.* The tripeptide KdPT protects from intestinal inflammation and maintains intestinal barrier function. *Am J Pathol.* **179**(3), 1230-1242 (2011).
25. Kemper, B. *et al.* Modular digital holographic microscopy system for marker free quantitative phase contrast imaging of living cells. *Proc. SPIE.* **6191** 61910T (2006).
26. Kemper, B., & von Bally, G. Digital holographic microscopy for live cell applications and technical inspection. *Appl Opt.* **47**(4), A52-61 (2008).
27. Langehanenberg, P., von Bally, G., & Kemper, B. Autofocusing in digital holographic microscopy. *3D Research.* **2**(1), 1-11 (2011).
28. Daimon, M., & Masumura, A. Measurement of the refractive index of distilled water from the near-infrared region to the ultraviolet region. *Applied optics.* **46**(18), 3811-3820 (2007).
29. Przibilla, S. *et al.* Sensing dynamic cytoplasm refractive index changes of adherent cells with quantitative phase microscopy using incorporated microspheres as optical probes. *J Biomed Opt.* **17**(9), 0970011-0970019 (2012).
30. Kemper, B. *et al.* Integral refractive index determination of living suspension cells by multifocus digital holographic phase contrast microscopy. *J Biomed Opt.* **12**(5), 054009 (2007).
31. Carpenter, A. E. *et al.* CellProfiler: image analysis software for identifying and quantifying cell phenotypes. *Genome Biol.* **7**(10), R100 (2006).
32. Marquet, P. *et al.* Digital holographic microscopy: a noninvasive contrast imaging technique allowing quantitative visualization of living cells with subwavelength axial accuracy. *Opt Lett.* **30**(5), 468-470 (2005).
33. Langehanenberg, P., Kemper, B., Dirksen, D., & von Bally, G. Autofocusing in digital holographic phase contrast microscopy on pure phase objects for live cell imaging. *Appl Opt.* **47**(19), D176-182 (2008).
34. Hanauer, S. B. *et al.* Maintenance infliximab for Crohn's disease: the ACCENT I randomised trial. *Lancet.* **359**(9317), 1541-1549 (2002).
35. Colombel, J. F. *et al.* Adalimumab for maintenance of clinical response and remission in patients with Crohn's disease: the CHARM trial. *Gastroenterology.* **132**(1), 52-65 (2007).
36. Feagan, B. G. *et al.* Vedolizumab as induction and maintenance therapy for ulcerative colitis. *N Engl J Med.* **369**(8), 699-710 (2013).
37. Sandborn, W. J. *et al.* Vedolizumab as induction and maintenance therapy for Crohn's disease. *N Engl J Med.* **369**(8), 711-721 (2013).
38. Monteleone, G. *et al.* Mongersen, an oral SMAD7 antisense oligonucleotide, and Crohn's disease. *N Engl J Med.* **372**(12), 1104-1113 (2015).
39. Vermeire, S. *et al.* Etrolizumab as induction therapy for ulcerative colitis: a randomised, controlled, phase 2 trial. *Lancet.* **384**(9940), 309-318 (2014).
40. Sandborn, W. J. *et al.* Ustekinumab induction and maintenance therapy in refractory Crohn's disease. *N Engl J Med.* **367**(16), 1519-1528 (2012).
41. Natividad, J. M. *et al.* Commensal and probiotic bacteria influence intestinal barrier function and susceptibility to colitis in Nod1-/-; Nod2-/- mice. *Inflamm Bowel Dis.* **18**(8), 1434-1446 (2012).
42. Melgar, S. *et al.* Validation of murine dextran sulfate sodium-induced colitis using four therapeutic agents for human inflammatory bowel disease. *Int Immunopharmacol.* **8**(6), 836-844 (2008).
43. Erben, U. *et al.* A guide to histomorphological evaluation of intestinal inflammation in mouse models. *Int J Clin Exp Pathol.* **7**(8), 4557-4576 (2014).
44. Bruckner, M. *et al.* Murine endoscopy for in vivo multimodal imaging of carcinogenesis and assessment of intestinal wound healing and inflammation. *J Vis Exp.* (90) (2014).
45. Zhao, K., Wang, W., Guan, C., Cai, J., & Wang, P. Inhibition of gap junction channel attenuates the migration of breast cancer cells. *Mol Biol Rep.* **39**(3), 2607-2613 (2012).
46. Pavillon, N. *et al.* Early cell death detection with digital holographic microscopy. *PLoS One.* **7**(1), e30912 (2012).
47. Hindryckx, P. *et al.* Clinical trials in ulcerative colitis: a historical perspective. *J Crohns Colitis.* **9**(7), 580-588 (2015).
48. Neurath, M. F., & Travis, S. P. Mucosal healing in inflammatory bowel diseases: a systematic review. *Gut.* **61**(11), 1619-1635 (2012).
49. Bryant, R. V., Winer, S., Travis, S. P., & Riddell, R. H. Systematic review: histological remission in inflammatory bowel disease. Is 'complete' remission the new treatment paradigm? An IOIBD initiative. *J Crohns Colitis.* **8**(12), 1582-1597 (2014).
50. Marchal Bressenot, A. *et al.* Review article: the histological assessment of disease activity in ulcerative colitis. *Aliment Pharmacol Ther.* **42**(8), 957-967 (2015).

